

# Efficient Control of Formation Flying Spacecraft

Michael Dellnitz, Oliver Junge, Arvind Krishnamurthy,  
Sina Ober-Blöbaum, Kathrin Padberg, Robert Preis

Department of Mathematics, University of Paderborn

**Abstract.** Several upcoming European and American space missions will be operated using a number of spacecraft flying in formation. The associated scientific challenges are demanding, both with respect to the construction of the spacecraft as well as to the mission design. For instance, energy efficient trajectories and corresponding control laws that enable precision formation flying over long periods of time have to be constructed. The stabilization of the group on its nominal trajectory has to be made robust with respect to failures of individual spacecraft. Correspondingly, robust and efficient inter-spacecraft communication topologies have to be designed. Finally, in view of visionary missions with hundreds of participating micro- or nano-satellites, geometric configurations have to be found which enable these communication topologies and which scale well with an increasing number of spacecraft. In this contribution we report on our investigations concerning these questions, in particular with respect to the design of energy efficient trajectories and robust communication topologies.

## 1 Introduction

Is there life in space? How did the planetary systems form? How unique is Earth as a planet within the universe? The European Space Agency (ESA) and the National Aeronautics & Space Administration (NASA) are currently investigating space missions with a number of spacecraft flying in formation in order to search for answers to these questions. Such missions are e. g. *DARWIN* [2] by ESA and *Terrestrial Planet Finder (TPF)* [21] by NASA. In these missions, the cooperative operation of several spacecraft exhibits a system with extended functionality – the group constitutes an infrared interferometer that will collect and analyze light reflected by distant planets.

The implementation of these missions – and future missions with an order of magnitude more spacecraft – poses a number of scientific challenges. Most notably, in light of the tight mass budget, energy efficient trajectories and control laws are sought that enable a frequent re-orientation of the group during its operation time. One particular advantage of multi-spacecraft missions is their potentially increased robustness with respect to failures of individual satellites. In order to realize this advantage, the procedure that stabilizes the group on its nominal orbit has to be formulated in a distributed manner and in such a way that a stable operation is guaranteed even when a certain number of spacecraft ceases to operate properly. One underlying mathematical question in this context is how to design a communication network that optimally supports the construction of this stabilizing control algorithm.

In this project we combine methods for the numerical investigation of dynamical and control systems with techniques from graph theory in order to develop

- methods for the design of energy efficient trajectories and control laws,
- scalable formation geometries and robust communication topologies,
- methods for the efficient reconfiguration of the formation geometry,
- algorithms and software for the real-time simulation of multi-spacecraft missions.

In this report, we will address the design of energy efficient trajectories and energetically optimal control laws, as well as the development of robust communication topologies. More precisely, this chapter is structured as follows:

In Section 2, we introduce the relevant mathematical model for formation flight. Section 3 is devoted to the design of energy efficient trajectories. In particular, we perform a global search in phase space with the aim to find regions that are dynamically stable in the sense that a small perturbation of some initial condition stays small under the uncontrolled dynamics, i.e. regions favorable for keeping formations in an energy efficient way.

Section 4 addresses the construction of optimal control laws for the reorientation of the formation. We present a new method for the computation of optimal control laws for mechanical systems that is based on a direct discretization of the underlying variational principle. We exemplarily apply this method in order to compute optimal control laws for the reorientation of a group of six spacecraft in a DARWIN-type mission. Via a hierarchical decomposition of the underlying optimal control problem we derive a distributed algorithm for its solution which is implemented and executed in parallel on basis of the library PUB [1].

An analysis of the robustness of different communication topologies is discussed in Section 5. In particular, we illustrate the dependence of the robustness of a certain topology in dependence on the number of failures of inter-spacecraft communication links.

We close with a summary of the results and a discussion on open topics and future work.

## 2 Modeling formation flight

In the vicinity of Earth, the motion of a spacecraft can be described by a three-body problem with Sun and Earth as *primary bodies*. By restricting the motion of Sun and Earth to circles and under the assumption that the spacecraft does not exert forces onto the primaries, one obtains the *circular restricted three body problem* (CRTBP) [20, 22], which, in rotating coordinates, reads

$$\begin{aligned}\dot{x} &= u, & \dot{u} &= 2v + x + c_1(x + \mu - 1) + c_2(x + \mu), \\ \dot{y} &= v, & \dot{v} &= -2u + y + (c_1 + c_2)y, \\ \dot{z} &= w, & \dot{w} &= (c_1 + c_2)z,\end{aligned}$$

where  $(x, y, z)$  is the position and  $(u, v, w)$  the velocity of the spacecraft with

$$c_1 = -\frac{\mu}{((x + \mu - 1)^2 + y^2 + z^2)^{3/2}}, \quad c_2 = -\frac{1 - \mu}{((x + \mu)^2 + y^2 + z^2)^{3/2}}. \quad (1)$$

Here

$$\mu = \frac{m_1}{m_1 + m_2} = 3.04043292 \times 10^{-6}$$

is the normalized mass of the Earth.

Note that although such a simplified model cannot account for all constraints, the CRTBP approximates the complex dynamics of the solar system more accurately than the traditionally used two-body problem, at least in the vicinity of a planet.

The CRTBP in rotating coordinates possesses five equilibrium points, the *Lagrange points*  $L_1, \dots, L_5$  (cf. Figure 1 for a sketch). Because of their vicinity to Earth  $L_1$  and  $L_2$  are of great interest. In particular, there exist families of periodic orbits, so called *Halo orbits*, about these Lagrange points which have been identified as convenient locations for certain types of missions. For instance, in the *Genesis Discovery Mission*, the natural dynamics of the CRTBP was exploited for the construction of energy efficient trajectories (in terms of fuel consumption) [9]. Also the upcoming missions like *DARWIN* or *TPF* are foreseen to operate in the vicinity of a Halo orbit around the  $L_2$  libration point.

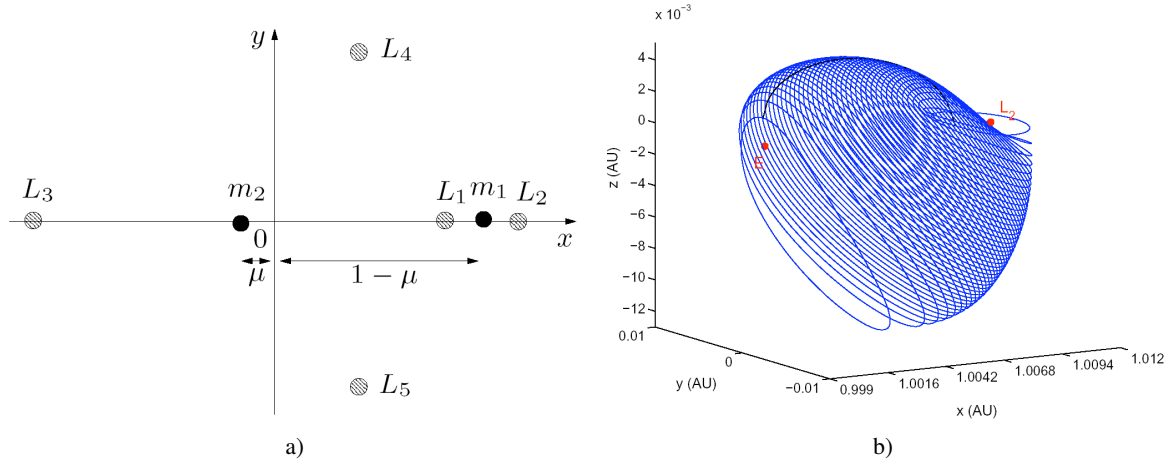


**Fig. 1.** a) The two primary bodies and the five Lagrange points (illustration [19]). b) Family of Halo orbits around  $L_2$  [10].

Our aim is now to identify Halo orbits or, more generally, regions in phase space, that are particularly appropriate for formation flight, in the sense that the natural dynamics supports the formation keeping. Once such a trajectory has been found, we develop control algorithms for formation-keeping and reconfiguration maneuvers with respect to this nominal trajectory.

### 3 Design of efficient trajectories

For the design of energy efficient trajectories for formation flights we exploit the natural dynamics of the CRTBP. The task is to identify regions in phase space that support formation keeping, i.e. regions where the distances between the spacecraft and their attitude change little under the natural dynamics when compared to other regions.

#### 3.1 Deformation analysis

In [10, 19] the average deformation of tetrahedral formations along Halo orbits has been analyzed. In this context, deformation is defined as the sum of the changes in the relative distances between the spacecraft under the natural, uncontrolled dynamics. Deformation has been computed with respect to initial values on the family of Halo orbits around  $L_2$  (see Figure 1) and by integrating the underlying differential equations for short time spans  $T = \frac{\pi}{300}$ , corresponding to 14 hours of flight time. The striking observation is that although Halo orbits near Earth are stable in the traditional sense (i.e. in the sense of Floquet theory), they exhibit a larger deformation over small time spans as orbits in the vicinity of  $L_2$ . In this sense the authors identified Halo orbits around  $L_2$  that are favorable for keeping formations in an energy efficient manner.

#### 3.2 Expansion rates

We now generalize the idea from the previous paragraph: in the dynamical systems context formation stability can be phrased as the requirement that a small perturbation in some initial condition remains small under the dynamics. To this end, in dynamical systems theory one typically uses infinitesimal concepts for the stability analysis.

To be more precise, let  $\dot{x} = f(x)$  be a smooth dynamical system,  $x \in \mathbb{R}^n$ . Let  $\varphi^t$  denote the flow, i.e.  $\varphi^t x_0$  solves the initial value problem w.r.t.  $x(0) = x_0$ . Then a small perturbation

$y = x_0 + \varepsilon$  in the initial condition evolves according to

$$\dot{\varepsilon} = Df(x_0)\varepsilon + \text{higher order terms.}$$

Note that  $D\varphi^t x_0$  with  $D\varphi^0 x_0 = I$  and  $x_0 = x(0)$  solves the *variational equation*  $\dot{\xi} = Df(x)\xi$ . So the linearization  $D\varphi^t x_0$  forms the basis for an analysis of the temporal evolution of small perturbations. The growth of these infinitesimal perturbations can be measured in terms of *expansion rates* (finite-time Lyapunov exponents):

$$\Lambda(T, x_0) := \frac{1}{2T} \log[\lambda_{\max}((D\varphi^T x_0)^\top D\varphi^T x_0)].$$

Expansion rates can be employed to characterize the short-term stability of regions in phase space as discussed in [16]. Note that  $\Lambda(T, x)$  is continuous in  $x$  for fixed  $T > 0$ .

### 3.3 Global exploration

Using the set-up described above, optimal regions for formation flight are those regions in phase space for which the expansion rate in the CRTBP (1) is small, i.e. approximately zero, for a given  $T > 0$ . We construct a box covering [4, 3, 5] of a large region around Earth and choose random initial conditions  $x$  in each box to compute  $\Lambda(T, x)$  for  $T = \frac{\pi}{300}$  (corresponding to 14 hours). For each box we save the minimal expansion rate with respect to initial conditions in that box. This procedure is computationally expensive because of its global nature. However, because of its natural parallelism all computations can be carried out in parallel. Moreover, the box covering is successively refined with boxes with high expansion rates being discarded, see Figure 2.

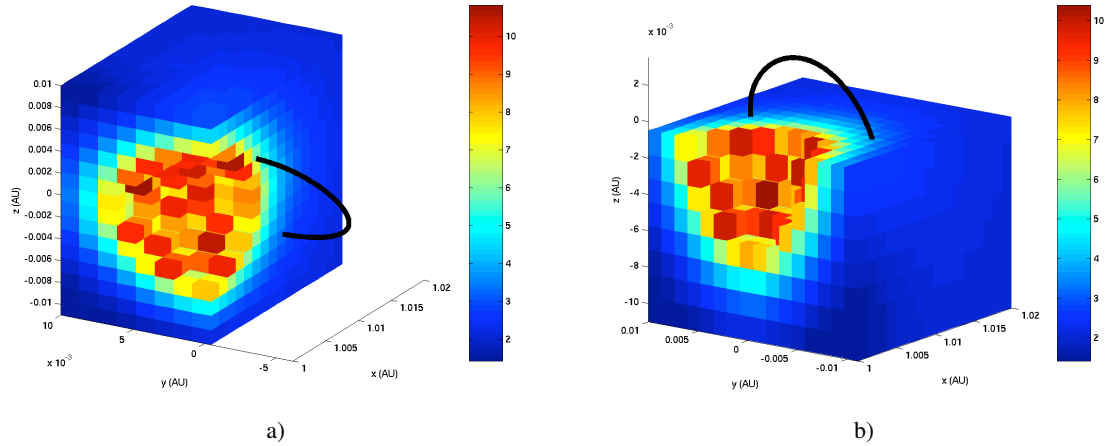


**Fig. 2.** Exploration of configuration space using expansion rates (projection into position space). Black: Halo orbit characterized by low deformation [10, 19].

### 3.4 Numerical Results

The global exploration based on a concept from dynamical systems theory (Figure 2) supports the results obtained in [10, 19]: we observe high expansion in the vicinity of Earth, which decreases when moving away from it towards  $L_2$ . We also find that formation flight without control

is not possible as  $\Lambda(T, x) \gg 0$  for all  $x$ . However, small expansion in the initial value is not the only requirement for an appropriate orbit, other mission constraints might be of equal importance. Figure 3 a) shows a trajectory with optimal expansion rate which is not adequate for deep-space observations. Moreover, the instantaneous stability typically varies along the orbit as demonstrated in Figure 3 b). Therefore, a global exploration as described above is only useful to obtain a good initial guess about appropriate regions in configuration space. For the actual mission design, it will be more promising to start with the mission constraints first and analyze for example a family of Halo orbits such as in [10, 19] or a family of quasi-periodic orbits (Lissajous orbits) with respect to expansion. For the remainder of this contribution we consider a Halo orbit around  $L_2$ .

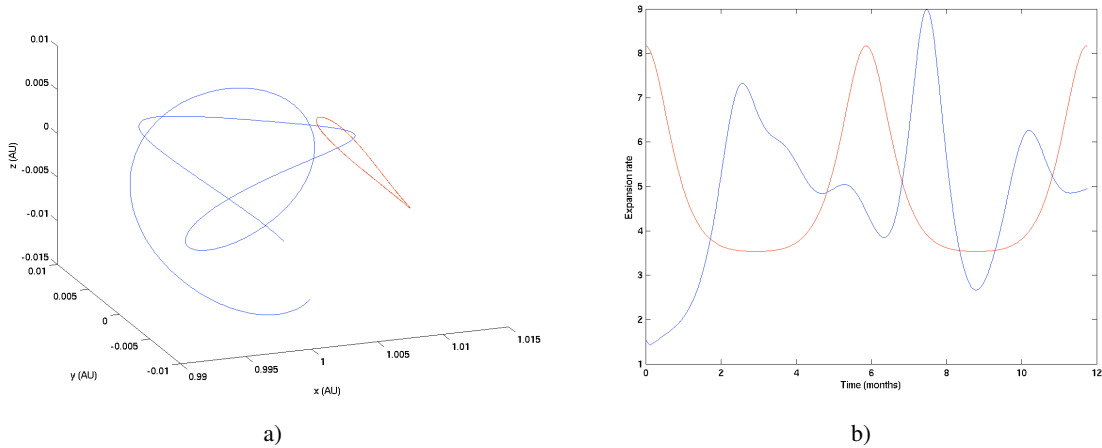


**Fig. 3.** a) Orbit w.r.t. initial condition chosen within the box having minimal expansion (blue) and Halo orbit as suggested in [10, 19] (red). b) Comparison of expansion rates along the two orbits (two periods of the Halo orbit).

## 4 Optimal control of formations

One of the many challenges of *DARWIN* [2, 13] and *TPF* [21] is to develop techniques for the control of a reconfiguration maneuver of the group of spacecraft. In light of the tight mass budget of these missions it is of great interest to minimize the propellant consumption in performing these reconfigurations. This problem can be formulated as an *optimal control problem*: A cost function has to be minimized with respect to the dynamics of the group of spacecraft.

The group is modeled as a mechanical system which describes the evolution of its states and includes external forces to control these states to the desired ones. The mechanical system can be described by a set of equations which provides constraints for the optimization problem.

### 4.1 The Control Method - DMOC

In order to solve such optimal control problems, we developed a new solution technique, called DMOC (*Discrete Mechanical Optimal Control*) [11], that relies on a direct discretization of a variational formulation of the problem:

A mechanical system with configuration space  $Q$  is to be moved along a curve  $q(t) \in Q$ ,  $t \in [0, 1]$ , from a state  $(q^0, \dot{q}^0) \in TQ$  to a state  $(q^1, \dot{q}^1) \in TQ$  under the influence of a force

$f \in T^*Q$ . The curves  $q$  and  $f$  shall minimize a given cost functional

$$J(q, f) = \int_0^1 C(q(t), \dot{q}(t), f(t)) dt. \quad (2)$$

Let  $L = K - V : TQ \rightarrow \mathbb{R}$  denote the Lagrangian of the mechanical system, where  $K$  is the kinetic energy and  $V$  the potential of the system. Then the motion  $q(t)$  of the system satisfies the *Lagrange-d'Alembert principle*, which requires that

$$\delta \int_0^1 L(q(t), \dot{q}(t)) dt + \int_0^1 f(t) \cdot \delta q(t) dt = 0 \quad (3)$$

for all variations  $\delta q$  with  $\delta q(0) = \delta q(1) = 0$ .

Using a global discretization of the states and the controls we directly obtain, via the *discrete Lagrange-d'Alembert principle*, equality constraints for the resulting finite dimensional nonlinear optimization problem as described next.

*Discretization.* We replace the state space  $TQ$  of the system by  $Q \times Q$  and a path  $q : [0, 1] \rightarrow Q$  by a *discrete path*  $q_d : \{0, h, 2h, \dots, Nh = 1\} \rightarrow Q$ ,  $N \in \mathbb{N}$ , where we view  $q_k = q_d(kh)$  as an approximation to  $q(kh)$  [15]. Analogously, we approximate the continuous force  $f : [0, 1] \rightarrow T^*Q$  by a discrete force  $f_d : \{0, h, 2h, \dots, Nh = 1\} \rightarrow T^*Q$  (writing  $f_k = f_d(kh)$ ).

Via an approximation of the action integral in (3) by a *discrete Lagrangian*  $L_d : Q \times Q \rightarrow \mathbb{R}$ ,

$$L_d(q_k, q_{k+1}) \approx \int_{kh}^{(k+1)h} L(q(t), \dot{q}(t)) dt,$$

and *discrete forces*

$$f_k^- \cdot \delta q_k + f_k^+ \cdot \delta q_{k-1} \approx \int_{kh}^{(k+1)h} f(t) \cdot \delta q(t) dt,$$

we obtain the *discrete Lagrange-d'Alembert principle* (4). This requires to find discrete paths  $\{q_k\}_{k=0}^N$  such that for all variations  $\{\delta q_k\}_{k=0}^N$  with  $\delta q_0 = \delta q_N = 0$ , one has

$$\delta \sum_{k=0}^{N-1} L_d(q_k, q_{k+1}) + \sum_{k=0}^{N-1} f_k^- \cdot \delta q_k + f_k^+ \cdot \delta q_{k+1} = 0, \quad (4)$$

which is equivalent to the *forced discrete Euler-Lagrange equations*

$$D_2 L_d(q_{k-1}, q_k) + D_1 L_d(q_k, q_{k+1}) + f_{k-1}^+ + f_k^- = 0, \quad k = 1, \dots, N-1. \quad (5)$$

In the same manner we obtain via an approximation of the cost functional (2) the *discrete cost functional*  $J_d(q_d, f_d)$ , such that we can formulate the *Discrete Constrained Optimization Problem* as

$$\min_{q_d, f_d} J_d(q_d, f_d) = \sum_{k=0}^{N-1} C_d(q_k, q_{k+1}, f_k, f_{k+1}) \quad (6)$$

subject to the discretized boundary constraints and the discrete Euler-Lagrange equations (5). This is a nonlinear optimization problem with equality constraints, which can be solved by standard optimization methods like SQP (*Sequential Quadratic Programming*).

## 4.2 Spacecraft Reconfiguration

We now apply DMOC to a reconfiguration maneuver for a DARWIN-type mission [12].

*The Model.* We deal with a group of  $n$  identical spacecraft. Each spacecraft is modeled as a rigid body with six degrees of freedom (position and orientation), i.e. the configuration manifold is  $SE(3)$ . We assume that each spacecraft can be controlled in this configuration space by a force-torque pair  $(F, \tau)$ , acting on its center of mass.

As mentioned before, it is planned in the current mission concepts for DARWIN and TPF to position the group of spacecraft in the vicinity of a Libration orbit around the  $L_2$  Lagrange point. Correspondingly, for each spacecraft the dynamical model for the motion of its center of mass is given by the circular restricted three body problem (1).

In a normalized, rotating coordinate system (cf. Figure 1), the potential energy of the spacecraft at position  $x = (x_1, x_2, x_3) \in \mathbb{R}^3$  is given by

$$V(x) = -\frac{1-\mu}{\|x - ((1-\mu), 0, 0)\|} - \frac{\mu}{\|x - (-\mu, 0, 0)\|}, \quad (7)$$

where  $\mu = m_1/(m_1 + m_2)$  is the normalized mass. Its kinetic energy is the sum of

$$K_{\text{trans}}(x, \dot{x}) = \frac{1}{2}((\dot{x}_1 - \omega x_2)^2 + (\dot{x}_2 + \omega x_1)^2 + \dot{x}_3^2) \quad \text{and} \quad K_{\text{rot}}(\Omega) = \frac{1}{2}\Omega^T J \Omega,$$

(assuming that its mass is equal to 1 for simplicity), where  $\Omega \in \mathbb{R}^3$  is the angular velocity and  $J$  the inertia tensor of the spacecraft.

*The Control Problem.* Our goal is to compute control laws  $(F_i(t), \tau_i(t))$ ,  $i = 1, \dots, n$ , for each spacecraft, such that the group moves from a given initial state  $(x_i, R_i, \dot{x}_i, \dot{R}_i)_{i=1}^n$ ,  $R_i \in SO(3)$ , into a prescribed target manifold within a prescribed time interval. In our application context, the target manifold will be defined by prescribing the relative positioning of the spacecraft, their common velocity as well as a common orientation. For their target state, we require the spacecraft to be located in a planar regular polygonal configuration with center on a Halo orbit. We additionally require the resulting controlled trajectory to minimize a given cost functional which typically is related to the associated fuel consumption of the spacecraft. Here we simply consider the cost function

$$J(F, \tau) = \sum_{i=1}^n \int_{t_0}^{t_f} |F_i(t)|^2 + |\tau_i(t)|^2 dt, \quad (8)$$

where  $F(t) = (F_1(t), \dots, F_n(t))$  and  $\tau(t) = (\tau_1(t), \dots, \tau_n(t))$  denote the force and torque functions for the system. Our optimal control problem consists of minimizing the functional (8) subject to the discrete Euler-Lagrange equations, the initial conditions and the constraints determining the target manifold.

## 4.3 Hierarchical Decomposition of the Problem and Parallelization

When one neglects collision avoidance concerns, the optimal control problem described in the previous section "almost" decouples the problem in the sense that the coupling only enters through the constraints on the final configuration. In this section, we show how one can exploit this fact in order to parallelize the associated computations.

*Hierarchical Optimal Control Problem.* The basic observation is that the problem can be formulated as a hierarchical optimization problem, where the *outer problem* relates to the correct arrangement of the final configuration and the  $n$  *inner problems* determine the optimal trajectory for one vehicle with fixed initial and final configuration, respectively.

We parameterize the final positions of the vehicles by the vector  $\varphi = (\varphi_1, \dots, \varphi_n)$ , where  $\varphi_i$  is the angle of vehicle  $i$ , determining the final position on a prescribed circle with prescribed center (cf. Figure 4). With this parameterization the problem can be formulated in the following

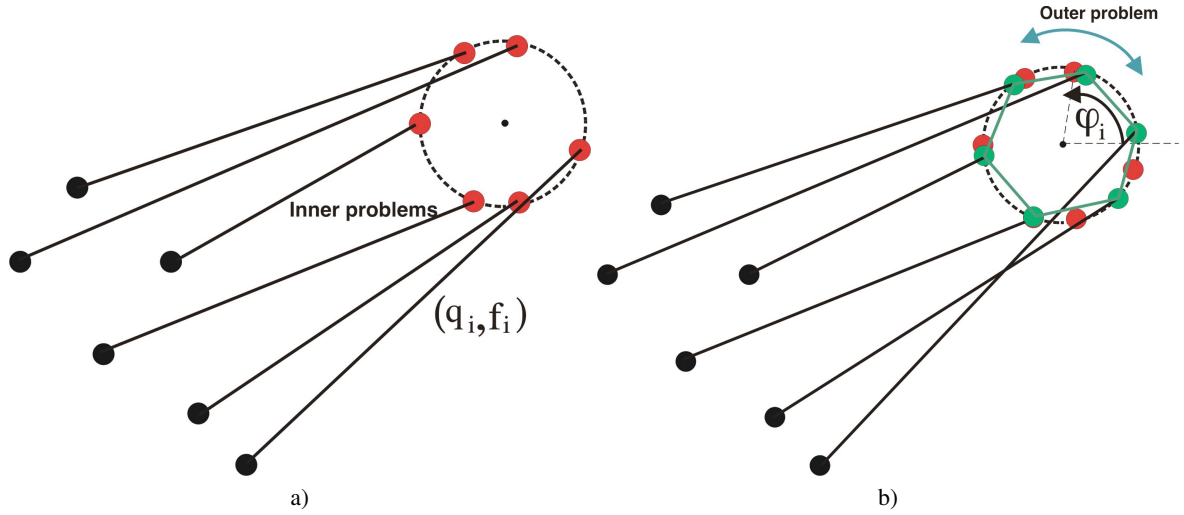


**Fig. 4.** Hierarchical optimal control problem. a) inner problem; b) outer problem.

hierarchical form:

$$\begin{aligned} \min_{\varphi} J(\varphi) &= \min_{\varphi} \sum_{i=1}^n \min \{J_i(q_i, f_i) \mid q_i : [0, 1] \rightarrow Q, f_i : [0, 1] \rightarrow T^*Q, \\ &\quad q_i(0) = q_i^0, \dot{q}_i(0) = \dot{q}_i^0, q_i(1) = q_i^f(\varphi_i), \dot{q}_i(1) = \dot{q}_i^f \\ &\quad \text{and } (q_i, f_i) \text{ fulfill the dynamics of vehicle } i\} \\ \text{subject to } &g(\varphi) = 0, \end{aligned}$$

where  $(q_i, \dot{q}_i)$  is the state,  $f_i$  the control force and  $J_i$  the cost function of vehicle  $i$ .  $g : S^n \rightarrow \mathbb{R}^n$  is a constraint function that guarantees a regular polygonal final configuration. The final positions  $q_i^f$  are parameterized by the angles  $\varphi_i$ ,  $i = 1, \dots, n$ , and the inner problems are uncoupled since each spacecraft has to minimize its costs separately subject to fixed initial and final states and its dynamics.

The outer problem includes the constraint for the final configuration, i.e. the coupling of the system. We use an iterative method (sequential quadratic programming) for the solution of both, the inner and the outer problems. In each step of the solution of the outer problem all  $n$  inner optimal control problems have to be solved again with new final positions on the circle.

*Parallelization.* The hierarchical structure of the problem enables a numerical computation in parallel, since we are faced with  $n$  uncoupled inner problems in each step of the solution of the outer problem. These  $n$  subproblems are solved in  $n$  different tasks. Our implementation uses the software package PUB [1] developed within the project A1. Each iteration step of the

outer optimization problem represents one *superstep*. After each superstep, the vehicles have to communicate during the *synchronization* of all processors.

We use the software package PUB for several reasons: Since our implementation involves more than one superstep we rely on a frequent communication between the processes (*"coupled parallel processes"*). Moreover, the computational time of each inner problem depends on the initial guess for the optimal trajectory. Therefore, it is of great interest to change load on the machines for an appropriate load balancing. These coupling and migration requirements can be easily realized in PUB [1].

#### 4.4 Numerical Results

We tested different kinds of models for the individual vehicles. Figure 5 a) depicts the optimal reconfiguration of six underactuated hovercraft in the plane. Since the final orientation of each vehicle is fixed, the optimal trajectories are large arcs instead of straight lines. In Figure 5 b) the final formation of a group of six spacecraft (modeled as rigid bodies) as the result of a reconfiguration maneuver along an  $L_2$  Halo orbit is shown.

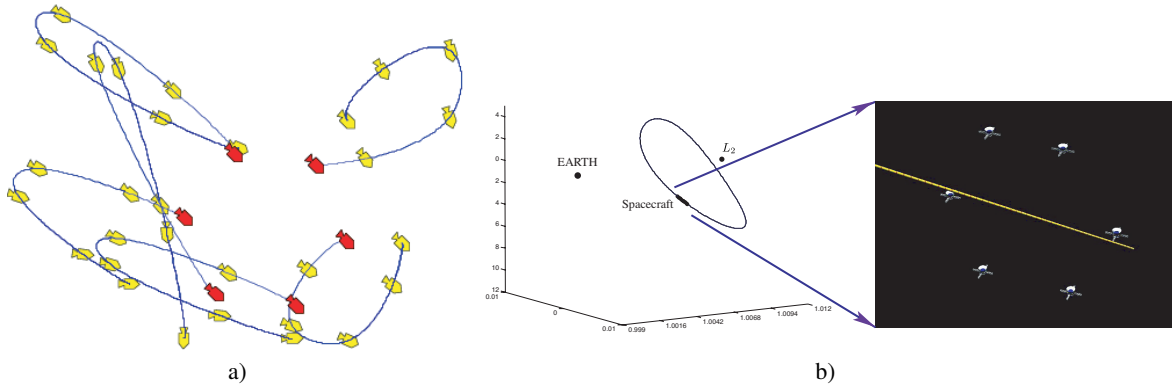


**Fig. 5.** Optimal reconfiguration of six vehicles: a) underactuated vehicles in the plane; b) modeled as rigid bodies along an  $L_2$  Halo orbit.

## 5 Robust communication topologies

As alluded to in the introduction, the communication between the spacecraft plays an important role in the design of robust stabilizing controls. In this section, we study the effect of changes in the communication graph on the stability of a certain feedback control law.

### 5.1 Dynamical Model

For this study, we model the dynamics of each of the  $N$  vehicles by a linear system

$$\dot{x}_i = Ax_i + Bu_i, \quad i = 1, \dots, N, \quad (9)$$

where  $x_i \in \mathbb{R}^6$  is the state and  $u_i \in \mathbb{R}^p$  for some  $p$  is the control of vehicle  $i$  and  $A$  and  $B$  are real matrices of appropriate size. As shown in [14], a linear local feedback can be designed which drives the system asymptotically into a prescribed formation, i.e. the vehicles attain prescribed

distances relative to each other as well as the same velocity. We follow [14] in the following description.

The feedback law is local in the sense that each vehicle  $i$  can generate its own control  $u_i$  from the determination of its state relative to the states of some subset  $S_i \subset \{1, \dots, N\}$  of all vehicles. Viewing the system as an undirected graph  $G = (V, E)$ , where the set of nodes  $V = \{1, \dots, N\}$  represent the vehicles and the set of edges  $E$  represent communication links (i.e.  $E = \{(i, j) : j \in S_i\}$ ), one can compactly write the entire system in the form

$$\dot{x} = \hat{A}x + \hat{B}\hat{F}\hat{L}(x - h). \quad (10)$$

Here  $x = (x_1, \dots, x_N) \in \mathbb{R}^{6N}$ ,  $\hat{A} = I_N \otimes A$ ,  $\hat{B} = I_N \otimes B$ ,  $\hat{F} = I_N \otimes F$ ,  $h = (h_1, \dots, h_N)$ ;  $h_i \in \mathbb{R}^6$  is some reference state for the  $i$ -th vehicle and  $\hat{L} = L \otimes I_6$ , with  $L$  being the Laplacian of the graph  $G$ , i.e.

$$L_{ij} = \begin{cases} 1 & : i = j \\ -\frac{1}{|S_i|} & : j \in S_i \\ 0 & : j \notin S_i. \end{cases} \quad (11)$$

We assume that all vehicles have identical dynamics and communication capabilities. So it seems natural to restrict the choice of communication graphs to those having a regular vertex degree. We consider an example with six spacecraft. Figure 6 depicts all non-isomorphic connected regular (undirected) graphs with six nodes (see e. g. [17]).

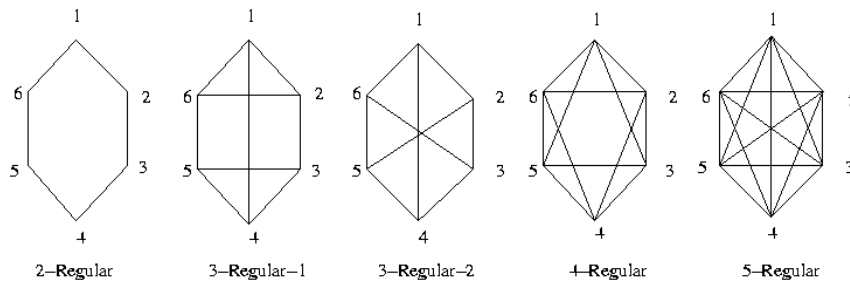


Fig. 6. All non-isomorphic connected regular undirected graphs with six nodes.

## 5.2 Robustness analysis

Robustness is the ability of a communication topology to ensure stability even with a certain number of link failures. Here we present two alternative approaches to analyze robustness, the minimal Laplacian eigenvalue analysis and the stability radius.

*Minimal eigenvalue analysis.* In [14] it is shown that the vehicles are in formation if and only if  $\hat{L}(x - h) = 0$ . Moreover, under certain assumptions, if the matrix  $A + \lambda BF$  is stable for each nonzero eigenvalue  $\lambda$  of  $L$ , then  $\hat{L}(x(t) - h) \rightarrow 0$  as  $t \rightarrow \infty$ , i.e. the vehicles asymptotically attain the desired formation. Using  $F = I_3 \otimes (f_1 \ f_2)$  as the feedback matrix, our goal will thus be to render the matrix

$$H_\lambda = \begin{pmatrix} 0 & 1 \\ 0 & a_{22} \end{pmatrix} + \lambda \begin{pmatrix} 0 & 0 \\ f_1 & f_2 \end{pmatrix}$$

stable for each nonzero eigenvalue  $\lambda$  of the Laplacian  $L$ . This matrix will be stable if and only if

$$a_{22} + \lambda f_2 < 0 \quad \text{and} \quad \lambda f_1 < 0,$$

i.e.  $f_1$  has to be chosen negative, since  $\lambda \in [0, 2]$  for all eigenvalues of  $L$ . If the single system dynamics is unstable, i.e.  $a_{22} > 0$ , then the smallest eigenvalue  $\lambda$  of  $L$  determines the choice of  $f_2$ . The minimal eigenvalues decrease when removing one or more edges from the corresponding graph (where we minimize over all possible removals while only considering connected graphs). It is interesting to monitor this decrease for an increasing number of communication links failures. Therefore, in Figure 7 we show for all graphs a sequence of the normalized minimal eigenvalues when up to four communication links fail. Notice that we do not consider the 2-regular graph as it becomes disconnected by removing just two edges. As expected, the full graph appears to be the most robust choice (Figure 7 a)), since it features the largest minimal nonzero eigenvalue and thus, for a fixed  $f_2$ , allows for the largest value for  $a_{22}$ . The full graph is also optimal if we choose  $f_2$  dependent on the graph and ask for maximal robustness with respect to communication link failures.

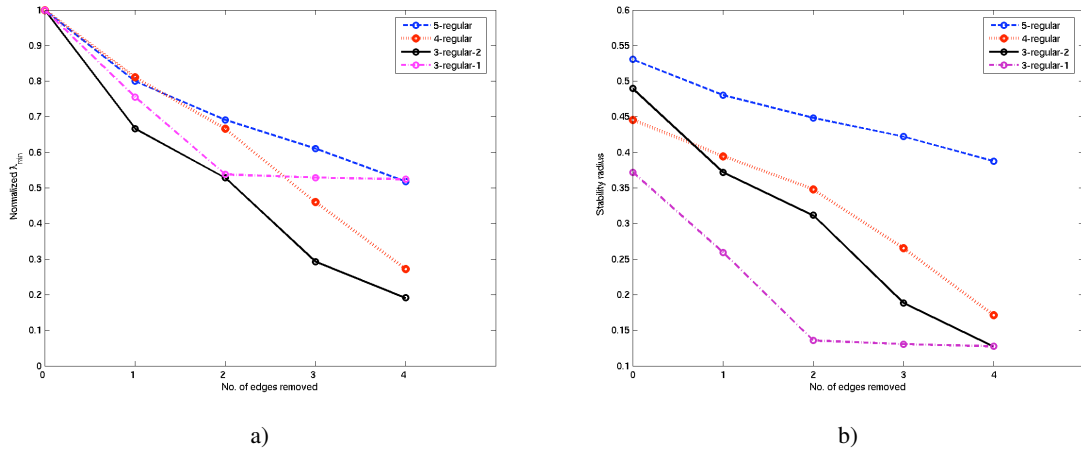


**Fig. 7.** a) Normalized minimal Laplacian eigenvalues for some communication link failures. b) The stability radii for some communication link failures.

*Stability Radius.* As an alternative, more systematic approach for robustness analysis, we propose to employ the concept of the *stability radius* from control theory, see [7].

We denote by  $\mathcal{U}_n$  the set of unstable real  $n \times n$  matrices:

$$\mathcal{U}_n = \{U \in \mathbb{R}^{n \times n} : \sigma(U) \cap \overline{\mathbb{C}_+} \neq \emptyset\},$$

where  $\overline{\mathbb{C}_+}$  is the closed right half complex plane. For a general matrix  $A \in \mathbb{R}^{n \times n}$ , the stability radius measures the distance  $r(A)$  of  $A$  from the set  $\mathcal{U}_n$  of unstable matrices.

From [8], the complex stability radius is given to be

$$r_{\mathbb{C}}(M) = \min_{w \in \mathbb{R}} s_n(iwI - M), \text{ where } s_n(A) = \min\{\|A - S\|, S \in \mathbb{R}^{n \times n}, 0 \in \sigma(S)\}.$$

Motivated by an adaptation of this notion to structured systems [8], we propose the following definition which is adapted to our context [6]. Let  $L(G)$  be the Laplacian associated with a given communication graph  $G = (V, E)$  and let  $\mathbb{L}(G)$  be the set of Laplacians associated with those graphs which result from  $G$  by removing some edges, i.e.  $\mathbb{L}(G) = \{L(G') : G' = (V, E'), E' \subset E\}$ . For some Laplacian  $L' = L(G') \in \mathbb{L}(G)$  with  $G' = (V, E')$  let  $d(L') = |E| - |E'|$  be the number of communication link failures. We define the stability radius of a given system  $(A, B, F, G)$  as

$$\overline{r}_{\mathbb{C}}(A, B, F, G) = \min_{\lambda \neq 0, \lambda \in \sigma(L(G))} r_{\mathbb{C}}(A + \lambda BF). \quad (12)$$

We computed this type of stability radius in dependence of the number of communication link failures for the same graph family as before (cf. Figure 7 b)). Here, the robustness of the five-regular graph is even more pronounced than in the minimal eigenvalue analysis. In both the analyzes presented above, we have an obvious result that the complete graph is the best choice. However, these are only two among several criteria for the choice of the communication structure. One can use a complete graph for six spacecraft, but for large numbers of spacecraft the complete graph would result in a very large number of communication facilities on each spacecraft and an enormous number of total communication links between the spacecraft. Both of these should be avoided and communication structures with a moderate vertex degree should be favored.

## 6 Discussion and Future Research

The techniques presented in this chapter provide promising first steps towards solutions to the challenges described in the introduction. Evidently, more work needs to be done in order to deliver a complete set of tools for the underlying mission design problem and in order to enable a realistic design and simulation of an example mission.

One important aspect that we did not touch upon when describing the construction of energy optimal reconfiguration maneuvers is how to avoid collisions between the spacecraft. While in principle there exists a variety of different approaches in order to incorporate this mission constraint into the model, these methods typically destroy the hierarchical structure of the optimal control problem as described in Section 4.3. A promising approach that avoids this drawback is to incorporate collision avoidance maneuvers “online”, i.e. to detect a close approach between two spacecraft during operation on their optimal trajectories and to initiate a collision avoidance maneuver only then. A major concern in this context would then be to ensure that the resulting collision free trajectories remain within certain bounds from the optimal solution energetically. On the theoretical side, an analysis of the convergence and energy conservation properties of DMOC needs to be carried out.

Our analysis of robust communication topologies has to be viewed as a very first step towards a complete understanding of this issue. In particular, a more systematic investigation of different graph classes needs to be performed. A particular promising type of graph for our application might be the “hierarchical layer graph” as proposed in [18]. Moreover, while in principle the linear dynamical model that we have been considering might be sufficient for our purposes (since the relative dynamics of the DARWIN resp. TPF-spacecraft in the vicinity of a Halo orbit can be sufficiently well approximated), we need to adapt the corresponding theory either to the time dependent framework or to a time discrete setting.

## 7 Theses in this project (chronological list)

### 7.1 Phd Theses

**Kathrin Padberg** ”Numerical Analysis of Transport in Dynamical Systems”, Universität Paderborn, 2005.

## References

1. O. Bonorden, M. Dynia, J. Gehweiler, and R. Wanka. PUB-library - user guide and function reference. *Release 8.1-pre*, 2003.

2. DARWIN. <http://sci.esa.int/science-e/www/area/index.cfm?fareaid=28>.
3. M. Dellnitz, G. Froyland, and O. Junge. The algorithms behind GAIO – set oriented numerical methods for dynamical systems. In *Ergodic Theory, Analysis, and Efficient Simulation of Dynamical Systems*, pages 145–174, 2001.
4. M. Dellnitz and A. Hohmann. A subdivision algorithm for the computation of unstable manifolds and global attractors. *Numerische Mathematik*, 75:293–317, 1997.
5. M. Dellnitz and O. Junge. Set oriented numerical methods for dynamical systems. In B. Fiedler, G. Iooss, and N. Kopell, editors, *Handbook of Dynamical Systems II: Towards Applications*, pages 221–264. World Scientific, 2002.
6. M. Dellnitz, O. Junge, A. Krishnamurthy, and R. Preis. Stable communication topologies of a formation of satellites. In *4th International Workshop on Satellite Constellations and Formation Flying*, 2005.
7. D. Hinrichsen and A.J. Pritchard. Stability radii of linear systems. *Systems and Control Letters*, 7:1–10, 1986.
8. D. Hinrichsen and A.J. Pritchard. Stability radius for structured perturbations and the algebraic riccati equation. *Systems and Control Letters*, 8:105–113, 1986.
9. K.C. Howell, B.T. Barden, R.S. Wilson, and M.W. Lo. Trajectory design using a dynamical systems approach with application to GENESIS. In *AAS/AIAA Astrodynamics Specialist Conference; AAS 97-709*, 1997.
10. O. Junge, J. Levenhagen, A. Seifried, and M. Dellnitz. Identification of halo orbits for energy efficient formation flying. In *International Symposium Formation Flying*, 2002.
11. O. Junge, J.E. Marsden, and S. Ober-Blöbaum. Discrete mechanics and optimal control. In *Proceedings of the 16th IFAC World Congress, Praha*, 2005.
12. O. Junge and S. Ober-Blöbaum. Optimal reconfiguration of formation flying satellites. *Accepted for IEEE Conference on Decision and Control and European Control Conference ECC, Seville, Spain*, 2005.
13. A. Karlsson and M. Fridlund. DARWIN. The infrared space interferometer, concept and feasibility study report. *ESA-SCI*, 2000.
14. G. Lafferriere, J. Caughman, and A. Williams. Graph theoretic methods in the stability of vehicle formations. In *American Control Conference*, 2004.
15. J.E. Marsden and M. West. Discrete mechanics and variational integrators. *Acta Numer.*, 10:357–514, 2001.
16. K. Padberg. Numerical analysis of transport in dynamical systems. Dissertation, Universität Paderborn, 2005.
17. R. Preis. *Analyses and Design of Efficient Graph Partitioning Methods*. Heinz Nixdorf Institut Verlagsschriftenreihe, 2000. Dissertation, Universität Paderborn, Germany.
18. C. Schindelhauer, T. Lukovszki, S. Rührup, and K. Volbert. Worst case mobility in ad hoc networks. *15th ACM Symposium on Parallel Algorithms and Architectures, SPAA*, pages 230–239, 2003.
19. A. Seifried. Formationsflug von Raumfahrzeugen. Diploma thesis, Universität Paderborn, 2003.
20. V. Szebehely. *Theory of orbits – The Restricted Problem of Three Bodies*. Academic Press, 1967.
21. Terrestrial Planet Finder. [http://planetquest.jpl.nasa.gov/tpf/tpf\\_index.cfm](http://planetquest.jpl.nasa.gov/tpf/tpf_index.cfm).
22. R. Thurman and A. Worfolk. The geometry of halo orbits in the circular restricted three-body problem. Technical Report GCG95, University of Minnesota, 1996.